

# Circularly Constrained Particle Motion in Spinning and Coning Bodies

D. L. MINGORI\*

University of California, Los Angeles, Calif.

AND

J. A. HARRISON†

Hughes Aircraft Company, El Segundo, Calif.

The motion of a particle constrained to move on a circular path within a body that is spinning and coning is examined. The equation governing this motion is expressed as a nonlinear, nonautonomous ordinary differential equation, and the behavior of solutions of this equation is investigated using phase plane techniques. Several classes of phase plane portraits are identified, and boundaries that separate system parameters giving rise to portraits of each class are established. Practical applications for the information thus generated include the analysis and design of certain passive balancing devices used to attenuate wobble in spinning spacecraft and the study of simplified models of nutation dampers and thermal control devices consisting of circular tubes partially filled with fluid.

## Nomenclature

$b$	= linear viscous friction constant
$l$	= distance from $O'$ to $O$
$N_1, N_2, N_3$	= inertially fixed axes
$O$	= point fixed in both carrier body and inertial space
$O'$	= center of circular path of particle
PS	= precession synchronous
$q$	= see Eq. (6)
$\bar{q}$	= see Eq. (16)
$r$	= radius of circular path of particle
SS	= spin synchronous
$V$	= see Eq. (6)
$\bar{V}$	= see Eq. (16)
$X_1, X_2, X_3$	= body fixed axes; $X_3$ is the desired spin axis (Fig. 1)
$X_1', X_2'$	= body fixed axes parallel to $X_1, X_2$ , respectively, lying in the plane of the particle motion (Fig. 1)
$\theta$	= particle rotation angle relative to carrier body (Fig. 1)
$\Lambda$	= rotation rate in carrier body of transverse component of $\omega$
$\mu_1, \mu_2, \mu_3$	= see Eq. (6)
$\bar{\mu}_1, \bar{\mu}_3$	= see Eq. (16)
$\tau$	= see Eq. (6)
$\bar{\tau}$	= see Eq. (16)
$\phi$	= angle between $N_3$ and $X_3$
$\Omega$	= magnitude of $X_3$ component of carrier body angular velocity (positive constant)
$\omega$	= inertial angular velocity of carrier body
$\omega_T$	= magnitude of transverse component of carrier body angular velocity (positive constant)

## Introduction

IN recent years, the performance requirements for spinning and dual-spin spacecraft have become increasingly difficult to satisfy. One important source of performance degradation is wobble due to static and dynamic unbalance in the rotating body. Several papers have dealt with ways of attenuating or eliminating the effects of unbalance; some proposing the introduction of passive flexible couplings to provide vibration

isolation,<sup>1,2</sup> and others proposing passive or active mechanisms to actually eliminate the unbalance.<sup>3-5</sup>

Passive devices capable of dissipating energy by internal relative motion can have a significant effect on the motion of spinning spacecraft. If the energy dissipated by these devices is not properly taken into account, instability may result.<sup>6</sup> To avoid this possibility, it is necessary to understand how the passive device will respond when the spacecraft is disturbed from a nominal state of pure spin. Knowledge of this response makes it possible to determine how much energy the device will dissipate for a given spacecraft motion, and this information is required to insure a stable design.

This paper is concerned with a passive balancing device of the type considered in Refs. 4 and 5. The system consists of four mass particles that rotate in circular paths perpendicular to and centered on the desired body fixed spin axis. The constrained motion of a typical particle is shown in Fig. 1. Three other particles move in similar circular paths with not more than two particles occupying the same plane. The present discussion will focus on the motion of a single balancer particle in response to spinning and coning of the carrier body. Behavior of the entire spacecraft system including all four

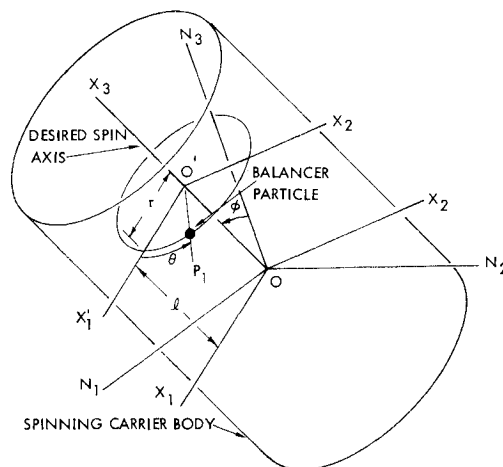


Fig. 1 Carrier body with typical balancer particle.

Received January 14, 1974; revision received May 1, 1974.

Index category: Spacecraft Attitude Dynamics and Control.

\* Associate Professor, Mechanics and Structures Department. Associate Fellow AIAA.

† Head, Dynamics Analysis Section, Guidance and Dynamics Department.

balancer particles will be examined in a subsequent paper based on Ref. 4. Information generated by considering a single particle plays an important role in understanding the behavior of the entire system.

Although the balancer system just described is emphasized in the discussion that follows, the results may be of value for understanding other systems as well. Reference 7 treats a "circular constraint nutation damper" consisting of a mass rotating about a body fixed axis on the end of a rod, and Ref. 8 treats a passive thermal control device consisting of a ring partially filled with fluid. In both cases, the equations describing the simplified mathematical models are essentially the same as those describing the motion of a single balancer particle.

### Mathematical Formulation

In practical applications, the mass of the balancer particles will be small compared to the total spacecraft mass. Hence, the effect of balancer motion on spacecraft motion will be small over short time intervals. During such time intervals, it can be assumed that the particles move essentially as if they were "driven" by the motion of the spinning body while the spinning body is not itself significantly affected by the particle motion. Suppose the carrier body is spinning and coning in free space with no external torques. For sufficiently large coning angles, the motion of an individual balancer particle will be essentially the same as that of a similarly constrained particle contained in a carrier body which spins and cones in a prescribed way about a point fixed in inertial space (point 0 in Fig. 1). In the discussion to follow, these observations and approximations will be used to arrive at a simplified mathematical model.

Let

$$\mathbf{T} = \omega_1 \mathbf{e}_1 + \omega_2 \mathbf{e}_2 + \omega_3 \mathbf{e}_3 \quad (1)$$

be the prescribed angular velocity of the carrier body in inertial space. The body fixed unit vectors  $\mathbf{e}_1, \mathbf{e}_2, \mathbf{e}_3$  are parallel to  $X_1, X_2, X_3$ , respectively. Assume that as the particle moves in its circular path, it experiences a viscous frictional force proportional to its velocity relative to the carrier body. A straightforward application of Newton's 2nd Law then yields the following governing equation for the particle

$$m\{\mathbf{r}(\ddot{\theta} + \dot{\omega}_3) - \mathbf{r}(\omega_2 \dot{\theta} + \omega_1 \dot{c}\theta)(\omega_1 \dot{\theta} - \omega_2 \dot{c}\theta) - l[(\dot{\omega}_2 + \omega_1 \omega_3)\dot{\theta} + (\dot{\omega}_1 - \omega_2 \omega_3)\dot{c}\theta]\} + b\dot{\theta} = 0 \quad (2)$$

where here and in the remainder of the paper

$$s(\ ) \equiv \sin(\ ); \quad c(\ ) \equiv \cos(\ ) \quad (3)$$

Suppose

$$\omega_1 = \omega_T c(\Lambda t); \quad \omega_2 = \omega_T s(\Lambda t); \quad \omega_3 = \Omega \quad (4)$$

These expressions for  $\omega_1, \omega_2$ , and  $\omega_3$  describe the motion of a freely rotating symmetric rigid body.  $\Lambda$  is the rate at which the transverse component of  $\omega$  rotates in the body containing the reference axes  $X_1, X_2, X_3$ . It can be positive or negative. This quantity is often referred to as the "nutation frequency" in aerospace applications.  $\omega_T$  and  $\Omega$  are always considered positive without loss of generality. Substitution of Eq. (4) into Eq. (2) yields

$$\ddot{\theta} + (b/rm)\dot{\theta} + (l/r)\omega_T(\Lambda + \Omega)s(\Lambda t - \theta) + \frac{1}{2}\omega_T^2 s[2(\Lambda t - \theta)] = 0 \quad (5)$$

This nonlinear, nonautonomous equation can be expressed in a more convenient form by introducing several new quantities. Let

$$\begin{aligned} \tau &\equiv |\Lambda|t; & q &\equiv \tau - (\Lambda/|\Lambda|)\theta \\ V &\equiv dq/d\tau; & \mu_1 &\equiv b/(rm|\Lambda|) \\ \mu_2 &\equiv l(\Lambda + \Omega)/r|\Lambda|; & \mu_3 &\equiv \omega_T/|\Lambda| \end{aligned} \quad (6)$$

$\mu_1$  may be interpreted as a damping parameter,  $\mu_2$  as a parameter related to the system configuration and nominal motion, and  $\mu_3$  as a parameter proportional to the coning angle  $\phi$  (Fig. 1). In terms of these quantities, Eq. (5) becomes

$$V dV/dq + \mu_1(V-1) - \mu_2\mu_3 s(q) - \frac{1}{2}\mu_3^2 s(2q) = 0 \quad (7)$$

The form of this equation suggests the application of phase plane techniques.

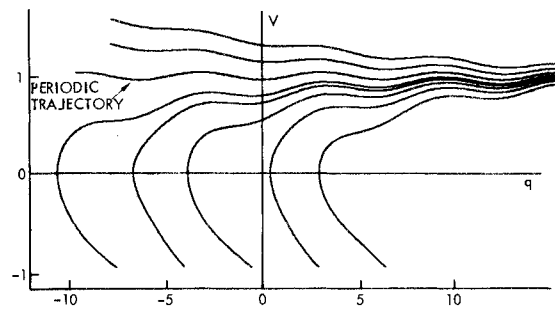


Fig. 2 Phase plane with no singular points.

### Phase Plane Analysis

Suppose  $\mu_1$  and  $\mu_2$  have fixed values and  $\mu_3$  is varied through a range of positive values. Physically, this amounts to studying the response of a given physical system for different coning angles. When  $\mu_3$  is sufficiently small, the phase plane trajectories corresponding to Eq. (7) will resemble those shown in Fig. 2. (These curves were generated by digital computer integration with  $\mu_1 = 0.1, \mu_2 = 2.0, \mu_3 = 0.02$ .) Singular points, i.e., points for which

$$V = 0 \quad (8)$$

and

$$\mu_1 + \mu_2\mu_3 s(q) + \frac{1}{2}\mu_3^2 s(2q) = 0 \quad (9)$$

do not exist because Eq. (9) has no real solutions. All trajectories approach asymptotically a trajectory in which  $V$  is a periodic function of  $q$  with an average value of 1. From Eq. (6) it follows that

$$V = dq/d\tau = 1 - (\Lambda/|\Lambda|)d\theta/d\tau \quad (10)$$

Hence, if the average value of  $V$  is 1, the average value of  $d\theta/d\tau$  is zero and the particle basically rotates in synchronism with the carrier body, the cone angle being too small to force the particle into synchronism with the precessional motion of the axis  $X_3$ . Following the terminology introduced by Cartwright et al.<sup>7</sup> for a closely related problem, periodic motion of the type depicted in Fig. 2 will be termed *spin synchronous* or more briefly, SS. [Reference 7 presents the results of an analytical and experimental study of a "circular constraint nutation damper" whose mathematical model is similar to that considered here. The particle motion is restricted to an inertially fixed plane, however, and as a result the last term in Eq. (7) is absent.]

As  $\mu_3$  becomes larger, it eventually reaches a value for which Eqs. (8) and (9) will have one solution (singular point) in each  $2\pi$  interval of  $q$ . (With  $\mu_1 = 0.1$  and  $\mu_2 = 2.0$ , this occurs when  $\mu_3 = 0.0502$ .) A typical phase plane diagram is shown in Fig. 3. Any further increase in the value of  $\mu_3$  will result in the appearance of additional singular points. Since the case depicted in Fig. 3 separates those cases in which singular points are present from those in which they are absent, it will be termed *critical case 1*.

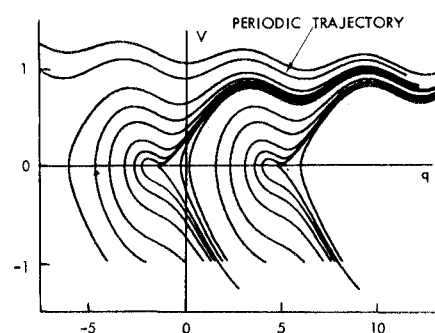


Fig. 3 Phase plane for critical case 1.

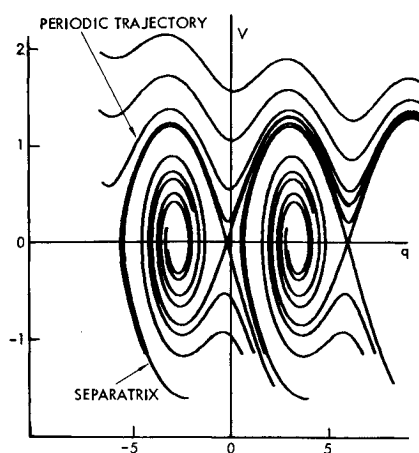


Fig. 4 Phase plane with singular points and periodic trajectory.

At each singular point,  $V = 0$  by definition. Hence, the motion corresponding to a singular point is one in which

$$d\theta/dt = \Lambda \quad (11)$$

[see Eqs. (6) and (10)]. To gain a better understanding of the nature of this motion, consider the plane  $P$  defined by the axes  $N_3$  and  $X_3$ . From the assumption that  $\omega$  as given in Eqs. (1) and (4) describes the motion of a freely rotating symmetric body, it follows that this plane rotates with a constant angular velocity parallel to  $N_3$ . The magnitude of this angular velocity is called the *precession frequency*. Let  $\mathbf{R}$  be a vector from point 0 to the particle  $p$  (see Fig. 1), i.e.,

$$\mathbf{R} = r c(\theta) \mathbf{e}_1 + r s(\theta) \mathbf{e}_2 + l \mathbf{e}_3 \quad (12)$$

and let  $\omega^{XP}$  be the angular velocity of the reference frame  $X$  defined by  $X_1$ ,  $X_2$ , and  $X_3$  relative to  $P$ . Again using the known behavior of a freely rotating symmetric body, it can be shown that

$$\omega^{XP} = -\Lambda \mathbf{e}_3 \quad (13)$$

Hence, the velocity of  $p$  relative to  $P$  becomes

$$\begin{aligned} \mathbf{V}^{pP} &= \frac{d}{dt} \mathbf{R} = \frac{d}{dt} \mathbf{R} + \omega^{XP} \times \mathbf{R} \\ &= -r s(\theta) \dot{\theta} \mathbf{e}_1 + r c(\theta) \dot{\theta} \mathbf{e}_2 \\ &\quad + (-\Lambda \mathbf{e}_3) \times [r c(\theta) \mathbf{e}_1 + r s(\theta) \mathbf{e}_2 + l \mathbf{e}_3] \\ &= [\Lambda - \dot{\theta}] r s(\theta) \mathbf{e}_1 - [\Lambda - \dot{\theta}] r c(\theta) \mathbf{e}_2 \end{aligned} \quad (14)$$

When Eq. (11) is satisfied,  $\mathbf{V}^{pP}$  becomes zero, i.e., the particle remains stationary relative to  $P$ . Motion corresponding to a singular point will therefore be called *precession synchronous*

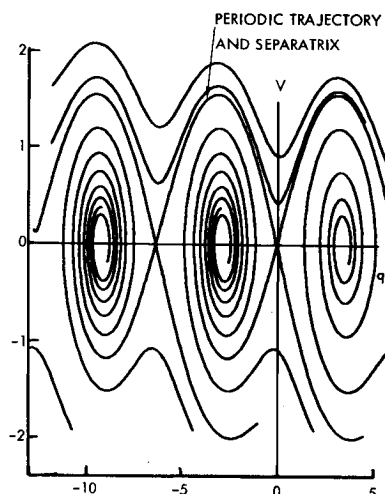
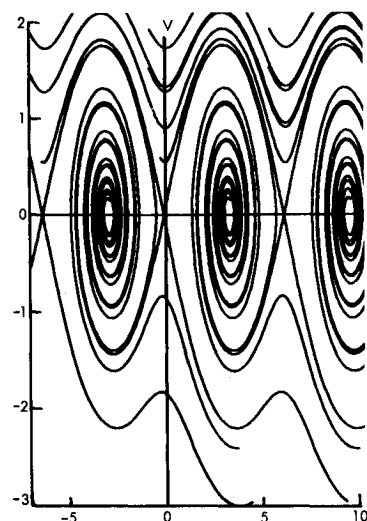


Fig. 5 Phase plane for critical case 2.

Fig. 6 Phase plane with no periodic trajectory; 2 singular points per  $2\pi$  interval.

or more simply PS. (This term has the same meaning as the term "nutation synchronous" used in Refs. 4 and 7.)

For a value of  $\mu_3$  slightly larger than that corresponding to critical case 1, two singular points, one a saddle and one a stable focus, appear in each  $2\pi$  interval of  $q$ . The periodic trajectory that was present for smaller values of  $\mu_3$ , however, will still remain if  $\mu_3$  is not too large. Figure 4 shows typical phase plane trajectories. It is clear that both spin synchronous and precession synchronous motions can be sustained, and that the eventual behavior of the particle depends on initial conditions.

As  $\mu_3$  is increased still further, the behavior illustrated in Fig. 5 is obtained. This occurs when  $\mu_3 = 0.3$  for the case presently under consideration ( $\mu_1 = 0.1$ ,  $\mu_2 = 2.0$ ). The oscillations of the periodic trajectory have increased in amplitude, and the minima of this trajectory have coalesced with the saddle points along the  $q$  axis. Also, those portions of the separatrices above the  $q$  axis have coalesced with the periodic trajectory, and the separatrices below this axis now enter the saddle points. If  $\mu_3$  is further increased a small amount, the resulting phase plane trajectories resemble those shown in Fig. 6. Here the periodic trajectories have disappeared and all trajectories tend toward precession synchronous motion. Because it represents a division between cases whose behavior exhibits important differences, the case illustrated in Fig. 5 is called *critical case 2*.

It has been pointed out that all trajectories in Fig. 6 eventually tend toward precession synchronous motion. This characteristic is common to all phase plane portraits with  $\mu_3$  larger than

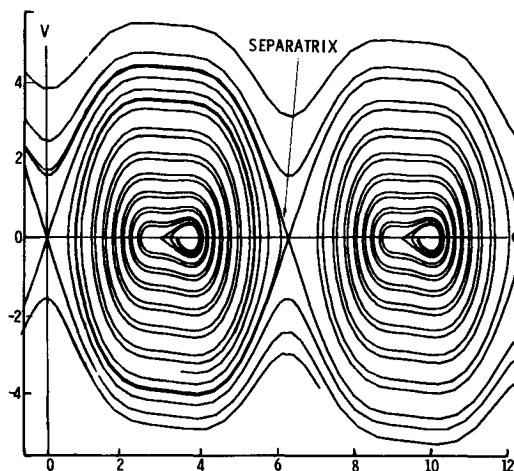
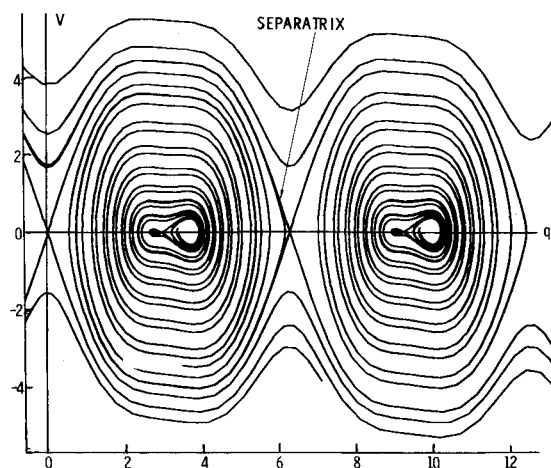


Fig. 7 Phase plane for critical case 3.

Fig. 8 Phase plane with 4 singular points per  $2\pi$  interval.

the value corresponding to critical case 2. For some practical applications,<sup>4,5</sup> this is by far the most important feature of these cases. However, a further subdivision of behavioral characteristics is also possible. This subdivision is based on the number of singular points that occur in a  $2\pi$  interval of  $q$ .

Consider Eq. (9). Suppose  $\mu_1$  and  $\mu_2$  have fixed values, and allow  $\mu_3$  to vary through a range of values for which singular points exist. When  $\mu_3$  is relatively small, the  $\sin q$  term will dominate the  $\sin 2q$  term and only 2 singular points will exist in each  $2\pi$  interval of  $q$ . When  $\mu_3$  becomes large, however, the  $\sin 2q$  term will become dominant, and 4 singular points will exist in each  $2\pi$  interval of  $q$ . For some intermediate value of  $\mu_3$ , therefore, a third critical case with three singular points must exist. With  $\mu_1 = 0.1$  and  $\mu_2 = 2.0$ , this occurs when  $\mu_3 = 2.265$ . The phase plane portrait for this case, *critical case 3*, is shown in Fig. 7.

Figure 8 displays a phase plane portrait with  $\mu_3$  larger than the value corresponding to critical case 3. The structure of the region surrounding a pair of stable foci is clarified in Fig. 9, an expanded and exaggerated version of part of Fig. 8. Note that the trajectory labeled (A) originating from saddle point (B) crosses the  $q$  axis to the right of saddle point (C). For larger values of  $\mu_3$ , this trajectory may cross to the left of saddle point (C) or even enter this point. The location of the crossing of trajectory (A) can be used to make further distinctions among cases in which four singular points occur. Because these distinctions have little significance with respect to the physical application that motivated this study, the calculations necessary to establish the boundaries of these subcases have not been carried out. Boundaries that indicate which combinations of spin synchronous or precession synchronous motions can occur, are of much greater importance.

### Results

Up to this point, the discussion has focused on changes in the phase plane portraits with variations in  $\mu_3$ ,  $\mu_1$ , and  $\mu_2$  being

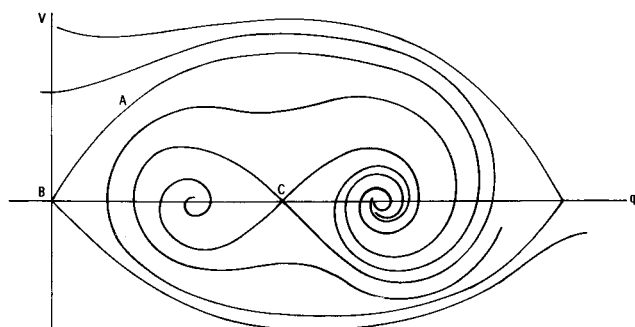
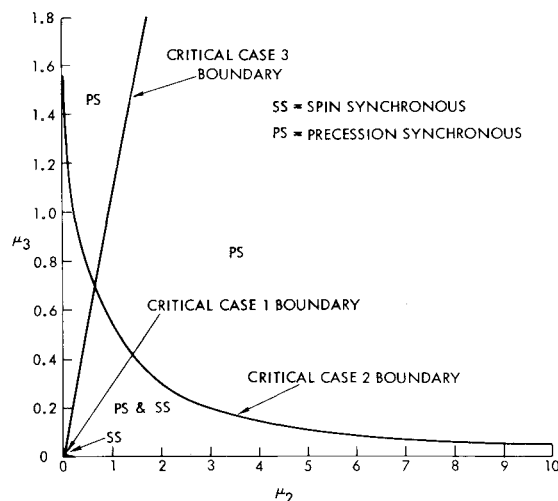
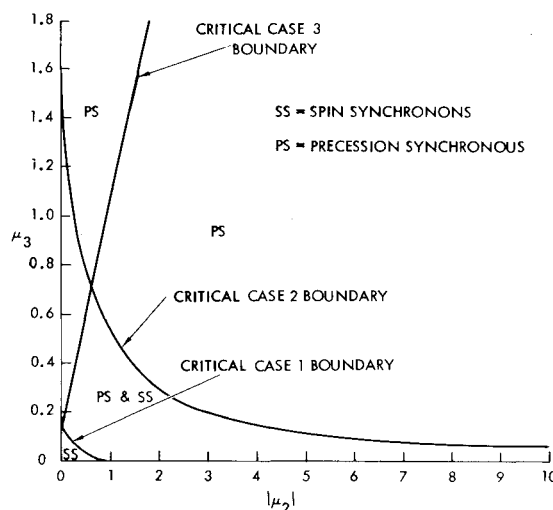


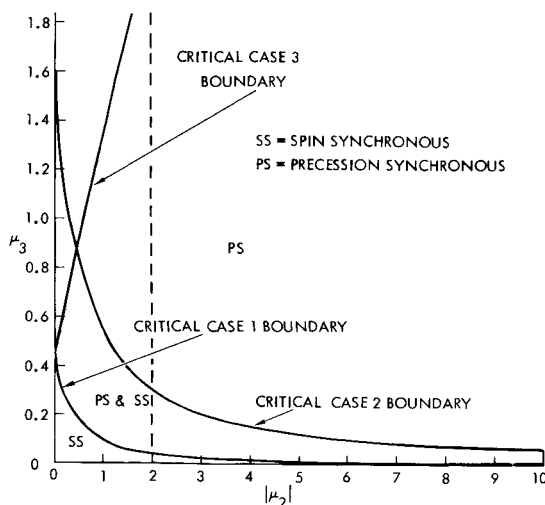
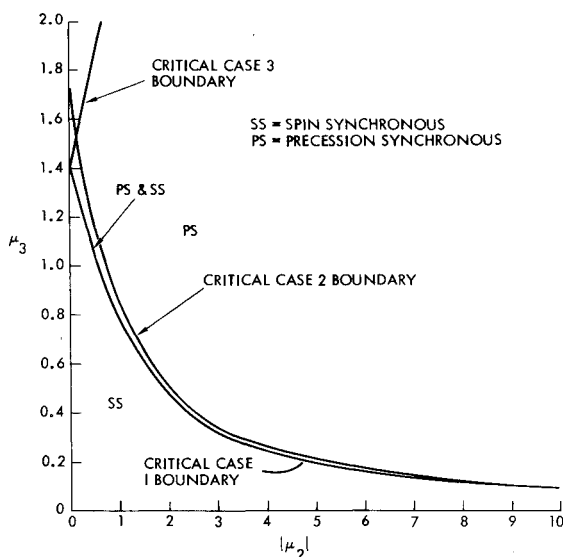
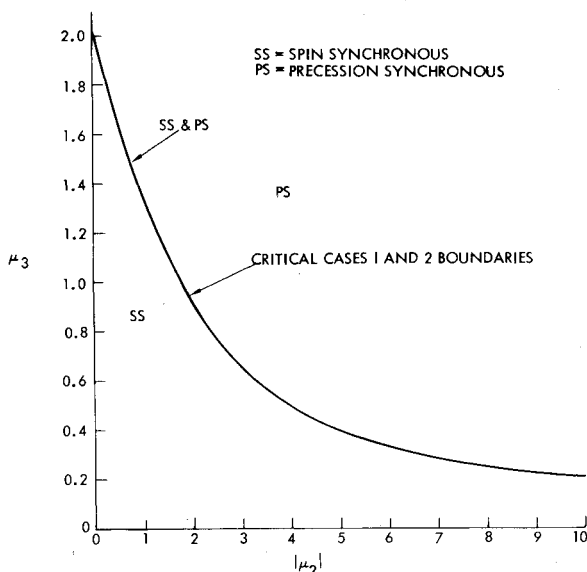
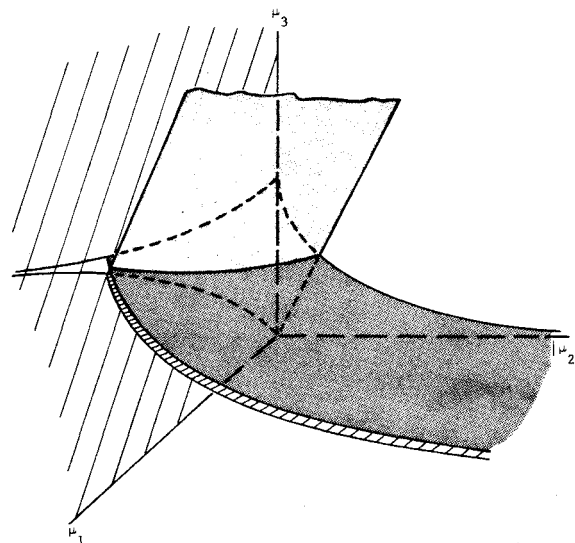
Fig. 9 Expanded diagram of Fig. 8 trajectory structure.

Fig. 10 Important regions in parameter space;  $\mu_1 = 0.001$ .

held fixed. Suppose both  $\mu_2$  and  $\mu_3$  are varied and only  $\mu_1$  is held fixed. It is then possible to locate curves in the  $\mu_2\mu_3$  plane that give rise to critical cases and separate regions of different behavioral characteristics. In the present study, this has been done by numerically integrating relatively large numbers of phase plane trajectories on a digital computer. The results are displayed in Figs. 10–14. Only the first quadrant is shown because for physical reasons,  $\mu_1$  and  $\mu_3$  can only take on positive values, and although  $\mu_2$  can be negative, the curves displayed in Figs. 10–14 are symmetric with respect to the  $\mu_3$  axis. The vertical dashed line in Fig. 12 refers to the values of  $\mu_1$  and  $\mu_2$  used for the earlier discussion and the development of Figs. 2–8. Proceeding upward from the  $|\mu_2|$  axis in each figure one passes first through a region in which there are no singular points and all motions approach spin synchronous motion. Then the critical case 1 boundary is crossed and a region is entered in which both spin synchronous and precession synchronous motions are possible. For still larger values of  $\mu_3$ , the critical case 2 boundary is crossed and all motions approach precession synchronous motions. The region above the critical case 1 boundary is divided into two portions by the critical case 3 line. To the right of this line, 2 singular points exist in each  $2\pi$  interval of  $q$ , and to the left, 4 singular points exist. A qualitative representation of the entire  $\mu_1, |\mu_2|, \mu_3$  space is shown in Fig. 15.

The plane  $\mu_2 = 0$  in Fig. 15 has a special significance that will be discussed briefly. It has been noted that the system studied in Ref. 7 is similar to that under consideration here. In

Fig. 11 Important regions in parameter space;  $\mu_1 = 0.01$ .


 Fig. 12 Important regions in parameter space;  $\mu_1 = 0.1$ .

 Fig. 13 Important regions in parameter space;  $\mu_1 = 1.0$ .

 Fig. 14 Important regions in parameter space;  $\mu_1 = 2.0$ .

 Fig. 15 Boundary surface in 3-dimensional parameter space.  $\mu_1 - |\mu_2| - \mu_3$  parameter space.

that investigation, the particle is constrained to move in a circular ring shaped tube whose inertial angular velocity is perpendicular to its plane, and whose center traces a circular path in inertial space. The plane of this path coincides with the plane of the tube, hence, all motion takes place in a single inertially fixed plane.

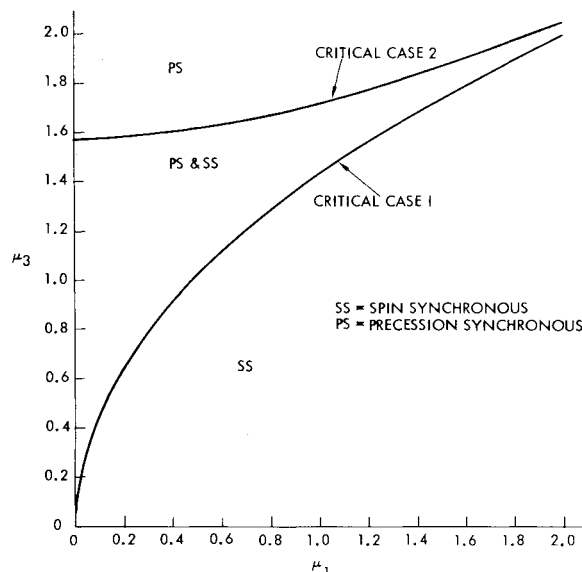
For the Ref. 7 system, the governing equation [i.e., the equation corresponding to Eq. (7) of the present work] assumes the form

$$\bar{V} d\bar{V}/d\bar{q} + \bar{\mu}_1(\bar{V} - 1) - \frac{1}{2}\bar{\mu}_3^2 \sin \bar{q} = 0 \quad (15)$$

Equation (7) reduces to the same form if  $\mu_2$  is set equal to zero and the following new symbols are introduced:

$$\begin{aligned} \bar{\tau} &= 2\tau; \quad \bar{q} = 2q, \quad \bar{V} = V \\ \bar{\mu}_1 &= \mu_1/2; \quad \bar{\mu}_3 = \mu_3/(2)^{1/2} \end{aligned} \quad (16)$$

Thus, the character of the phase plane portraits for Eq. (15) can be determined by examining the  $\mu_2 = 0$  plane in Fig. 15. This plane is reproduced in a more useful form in Fig. 16. For given values of  $\bar{\mu}_1$  and  $\bar{\mu}_2$  in Eq. (15), locate the point in Fig. 16 whose coordinates are  $(\bar{\mu}_1, \bar{\mu}_2) = [2\bar{\mu}_1, (2)^{1/2}\bar{\mu}_3]$ . The phase plane portrait for Eq. (15) will have the character indicated by this point. If precession synchronous motion is indicated, 2 singular


 Fig. 16 Important regions in parameter space;  $\mu_2 = 0$ .

points will occur in each  $2\pi$  interval of  $\bar{q}$ . It is worth pointing out that for parameter values lying between the critical case 1 and critical case 2 curves, both spin synchronous and precession synchronous motion can occur and the nature of the motion for large times depends on initial conditions. This possibility is not reported in Ref. 7 which indicates that only one class of motions, either spin synchronous or precession synchronous, can occur for a given set of parameters, and that large time behavior is independent of initial conditions.

### References

- <sup>1</sup> Cretcher, C. K. and Mingori, D. L., "Nutation Damping and Vibration Isolation in a Flexibly Coupled Dual-Spin Spacecraft," *Journal of Spacecraft and Rockets*, Vol. 8, No. 8, Aug. 1971, pp. 817-823.
- <sup>2</sup> Wenglarz, R. A., "Dynamically Unbalanced Dual-Spin Space

Stations with Rigid or Low-Coupling Interconnections," *Journal of Spacecraft and Rockets*, Vol. 8, No. 10, Oct. 1971, pp. 1032-1037.

<sup>3</sup> Lorell, K. R. and Lange, B. O., "An Automatic Mass-Trim System for Spinning Spacecraft," *AIAA Journal*, Vol. 10, No. 8, Aug. 1972, pp. 1012-1015.

<sup>4</sup> Harrison, J. A., "A Device for Automatically Balancing a Spinning Spacecraft," Ph.D. thesis, July 1972, University of California, Los Angeles, Calif.

<sup>5</sup> Martz, W. C. and Grantham, C., "A Passive Balancer for a Class of Rotating Spacecraft," TN D-6924, Oct. 1972, NASA.

<sup>6</sup> Likins, P. W., "Attitude Stability Criteria for Dual Spin Spacecraft," *Journal of Spacecraft and Rockets*, Vol. 4, No. 12, Dec. 1967, pp. 1638-1643.

<sup>7</sup> Cartwright, W. F., Massingill, E. C., and Trueblood, R. D., "Circular Constraint Nutation Damper," *AIAA Journal*, Vol. 1, No. 6, June 1963, pp. 1375-1380.

<sup>8</sup> Alfrend, K. T. and Hubert, C., "The Stability of a Dual-Spin Satellite with Two Dampers," *Journal of Spacecraft and Rockets*, Vol. 11, No. 7, July 1974, pp. 469-474.